Available online at www.sciencedirect.com
SCIENCE DIRECT®
Biochemical Pharmacology 68 (2004) 2443–2450
Biochemical Pharmacology
www.elsevier.com/locate/biochempharm

The interactions between the N-terminal and C-terminal domains of the human UDP-glucuronosyltransferases are partly isoform-specific, and may involve both monomers

Mika Kurkela[a], Jouni Hirvonen[a,b], Risto Kostiainen[a,b], Moshe Finel[a,*]

[a]*Viikki DDTC, University of Helsinki, P.O. Box 56 (Viikinkaari 5E), 00014 Helsinki, Finland*
[b]*Faculty of Pharmacy, University of Helsinki, P.O. Box 56 (Viikinkaari 5E), 00014 Helsinki, Finland*

Received 18 June 2004; accepted 9 August 2004

Abstract

The pathological mutation Y486D was previously shown to reduce the activities of the UDP-glucuronosyltransferases (UGTs) 1A1 and 1A6 by about 88% and 99%, respectively. Surprisingly, the corresponding mutation in UGT1A9 (Y483D) doubled the V_{max} of scopoletin glucuronidation, whereas the entacapone glucuronidation rate was decreased by about 50%. Due to the primary structure identity of the C-terminal half of all the human UGTs of the 1A subfamily, the sharp differences between them in the effect of a mutation deep inside the C-terminal half suggested that there are isoform-specific interactions between the variable N- and the conserved C-terminal halves. In dimeric enzymes, like the UGTs, such interactions might either occur within the same polypeptide, or between opposite monomers. The latter implies functional monomer–monomer interactions, and this was investigated using hetero-dimeric UGTs. Insect cells were co-infected with mixtures containing different combinations of recombinant baculoviruses encoding either UGT1A4 or 1A9Sol. The UGT1A4 was selected because it glucuronidates neither entacapone nor scopoletin at significant rates. The active enzyme in these hetero-dimers was 1A9Sol, a truncation mutant of UGT1A9 that exhibited a very low ratio of entacapone to scopoletin glucuronidation rates. Interestingly, the ratio of entacapone to scopoletin glucuronidation rates in the co-infected cells was dependent on, and markedly increased with, the probability that 1A9Sol forms hetero-dimers with UGT1A4. In addition, the apparent K_m for entacapone in the hetero-dimers was much lower than in 1A9Sol, and resembled the corresponding value in full-length UGT1A9. The results, thus, revealed important monomer–monomer interactions within the UGTs.

Keywords: Glucuronidation; Drug metabolism; Protein–protein interactions; Dimer; Monomer

1. Introduction

The UDP-glucuronosyltransferases (UGTs) are membrane-bound proteins of the endoplasmic reticulum that play important roles in the metabolism of xenobiotics and endobiotics. The UGTs catalyse glucuronic acid transfer from UDP-glucuronic acid (UDP-GA) to aglycones that are mostly small lipophilic compounds, including endogenous molecules like bilirubin and steroids, carcinogens from the environment, and many drugs or drug metabolites [1–4]. The human genome contains about 16 functional UGT genes that are divided into two main subfamilies, UGT1A and UGT2B [3]. At the protein level, the UGTs seem to be composed of two major domains of rather similar size, the relatively variable N-terminal half, and the highly conserved C-terminal half. Furthermore, due to exon sharing in the UGT1A gene locus, the C-terminal halves of all the members of the UGT1A subfamily are identical [3]. The aglycone specificity of individual UGTs appears, therefore, to be determined by the N-terminal domain, while the binding site of the sugar donor, UDP-glucuronic acid, is probably located primarily within the C-terminal domain. Nevertheless, this division of labour may be superficial, since the UGTs are dimeric [5–9], and monomer–monomer interactions may affect substrate binding. Little is presently known, however, on the interactions between the monomers within the dimeric UGTs.

Abbreviations: CN-II, Crigler–Najjar syndrome type II; UGTs, UDP-glucuronosyltransferases; UDP-GA, UDP-glucuronic acid

* Corresponding author. Tel.: +358 9 191 59193; fax: +358 9 191 59556.
E-mail address: moshe.finel@helsinki.fi (M. Finel).

0006-2952/$ – see front matter © 2004 Elsevier Inc. All rights reserved.
doi:10.1016/j.bcp.2004.08.019

The UGTs are bound to the endoplasmic reticulum membrane so that most of their mass is located on the lumenal side of the membrane. A short trans-membrane segment is present close to the C-terminus of these 50–60 kDa proteins, and the last 20–26 amino acids are exposed on the cytoplasmic side of the membrane [1]. We have recently demonstrated that the UGT1A9 is an exception among the human UGTs in its resistance to inhibition by Triton X-100 solubilization [9]. The identity of the C-terminal half among all the human UGTs of the 1A subfamily implies that the differences in detergent sensitivity between the UGT1A9 and the other human UGTs arise from residues within the N-terminal half. On the other hand, the likely binding of detergent micelle(s) to the single trans-membrane helix, as well as the removal of the trans-membrane helix, together with the cytoplasmic tail, affect the activity of the truncation mutant [10], suggesting that the fully identical C-terminal half of the enzyme is involved in the variable detergent sensitivity of the UGTs. This apparent contradiction may be explained by protein–protein interactions between the two major domains of the UGTs. It thus appears that the interactions between the N- and C-terminal domains may play an important role in the structure and perhaps also in the function of the UGTs.

The pathological Y486D mutation in UGT1A1 causes Crigler–Najjar syndrome type II (CN-II) [11,12], and it severely lowers the activity of both UGTs 1A1 and 1A6 [13,14]. This mutation changes the Tyr residue in the highly conserved QYHSLDV segment, and the last Val in this sequence is the first in the stretch of 17 hydrophobic amino acids that form the trans-membrane helix. Interestingly, the DV in this segment is the point where previous attempts to generate water-soluble UGTs, by truncating the human UGT1A6, or the rat UGT2B1, failed [15,16]. We have, nevertheless, truncated UGT1A9 at exactly the same point and in this case the mutant, 1A9Sol, was active and water-soluble [10]. The latter results raised the possibility that a corresponding Y to D mutation in UGT1A9 might not be detrimental to enzymatic activity, thereby revealing isoform-specific differences in the sensitivity to a mutation within the C-terminal half. We have, therefore, generated the equivalent of the 1A1/Y486D mutant in UGT1A9, namely 1A9/Y483D, and analysed its scopoletin and entacapone glucuronidation activities. In addition, we have examined heterodimers containing the truncation mutant of UGT1A9, 1A9Sol, together with the full-length UGT1A4. The results reveal extensive protein–protein interactions within the UGTs.

2. Materials and methods

Scopoletin, saccharolactone, and UDP-GA were purchased from Sigma. Entacapone was kindly provided by Orion Pharma (Espoo, Finland), scopoletin and entacapone glucuronides were synthesised in our laboratory [17]. Restriction enzymes were purchased from New England Biolabs and from MBI Fermentas.

2.1. Gene manipulation and mutant expression in insect cells

Generation of recombinant baculovirus and expression optimisation were done as previously described [9], except that the insect cells were cultured in HyQ® SFX-Insect medium (HyClone) supplemented with 5% foetal bovine serum. Co-infection of insect cells with UGT1A4 and 1A9Sol was performed as follows: SF9 insect cells were collected in the logarithmic growth phase, re-suspended to a 2×10^6 cells/ml of fresh medium, and infected with a mixture (3 μl/ml cell suspension) containing different portions of recombinant baculoviruses that drive the expression of either UGT1A4 or 1A9Sol. The cells were collected at 48 h post-infection, washed once with phosphate buffered saline and stored at −20 °C for up to 2 weeks. Frozen cells were thawed, suspended in 1 ml of cold H_2O and mixed thoroughly. In contrast to the regular assays with membrane-bound UGTs, in the case of cells co-infected with 1A9Sol and UGT1A4, the mixture of the washed, frozen and thawed cells, rather than the membrane fractions, was subjected directly to the activity assays.

2.2. Activity and analytical assays

The UGT activity was assayed using 50 mM phosphate buffer (pH 7.4), 10 mM $MgCl_2$, 5 mM saccharolactone, 5 mM UDP-GA, and 500 μM aglycone substrate (unless otherwise stated), and the reaction volume was 100 μl. The assays were performed at 37 °C and the incubation times were 45 min for 1A9Sol and the co-infection samples, and 20 min for the UGT1A9 or 1A9/Y483D samples. The reactions were terminated by the addition of 10 μl of 4 M perchloric acid, chilling on ice and centrifugation [9]. The resulting glucuronides were separated from the aglycones and quantified using an Agilent 1100 series HPLC equipment. The entacapone glucuronide was separated by Hypersil BDS C18150 × 4.6 mm column (Hewlett-Packard) with 42% methanol in 50 mM phosphate buffer at pH 3. The flow rate of the mobile phase was 1 ml/min, and the detection wavelength was 310 nm. The scopoletin glucuronide was separated by Chromolith SpeedROD RP-18e 50 × 4.6 mm column (Merck) with mobile phase of 10% methanol in 50 mM phosphate buffer at pH 3. The flow rate was 0.8 ml/min for 4.5 min, after which it was increased to 2.5 ml/min over 0.5 min and held constant for 5 min, then reduced back to 0.8 ml/min over 1 min. Fluorescence was measured at 335 nm excitation/455 nm emission. The kinetic parameters were calculated by fitting the experimental data to the Michaelis–Menten equation in either its basic form, $v = V_{max} \times S/(K_m + S)$, or with

substrate inhibition, $v = V_{max}/(1+ (K_m/S) + (S/K_i))$, using SigmaPlot (enzyme kinetics module 1.1).

2.3. Miscellaneous

Protein concentrations were measured by the bicinchoninic acid system (Pierce) using bovine serum albumin as a standard. The relative expression levels of UGT1A9 (1A9-XHC, [9]) and 1A9/Y483D were estimated by Dot blot analyses in which the membrane samples were first diluted to 1 mg of protein per ml in the presence of SDS (final concentration 1%), and mixed well. Aliquots of this mixture, 2 or 3 μl, were mixed with 4 μl of SDS-PAGE sample buffer, supplemented with 2-mercapto-ethanol and spotted on a nitrocellulose membrane. The membrane was then baked at 80 °C for 30 min, followed by 15 min wash in 25 mM Tris, 192 mM glycine, 20% (v/v) methanol, and 0.1% SDS (our standard electro-blotting buffer), and immersed in skimmed milk for 16 h at 4 °C. The His-tagged UGTs were visualized by chemiluminescence detection (SuperSignal, Pierce) using Tetra-His monoclonal antibodies (Qiagen) as primary antibodies and goat anti-mouse IgG-HRP (Santa Cruz Biotechnology) as secondary antibodies. The blots were analysed using chemiluminescence detector, GeneGnome (Syngen), and its software.

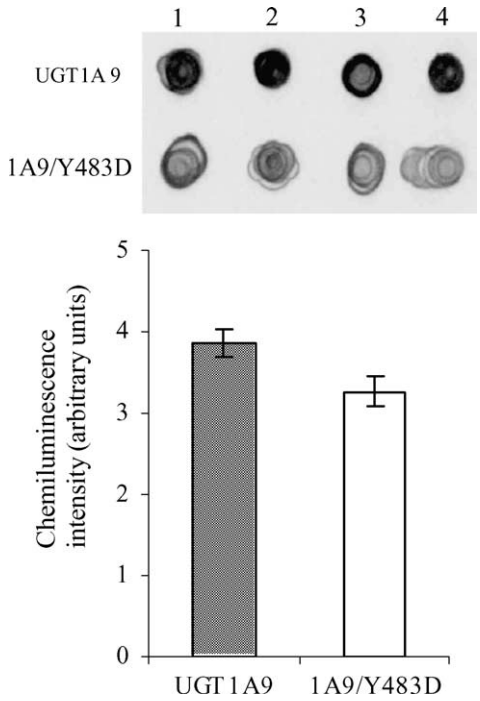

Fig. 1. Comparison of the expression level of UGT1A9 and the mutant 1A9/Y483D in the membrane samples. Membranes from insect cells expressing each enzyme were examined by Dot blot using monoclonal antibodies against their C-terminal His-tag (see Section 2 for further details). A "negative picture" of the recorded chemiluminescence is shown in the upper panel, and the outcome of the analyses is presented in the lower panel.

3. Results

The Y486D mutation in UGT1A1 affects the highly conserved Tyr residue that is located in the vicinity of the trans-membrane helix near the C-terminus of the protein. The mutation causes CN-II, and inhibits the activity of UGTs 1A1 and 1A6 [14]. The mode of exon sharing that governs the transcription of all the UGTs of the 1A subfamily implies that these CN-II patients carry analogous mutants of the other UGT1A enzymes. We have now generated the corresponding mutation in UGT1A9, namely 1A9/Y483D, and expressed the mutant in baculovirus-infected insect cells. The membrane fraction of the cells was isolated and employed in the subsequent activity and kinetic studies. It may be noted here that most of the UGTs that we have previously expressed in baculovirus-infected insect cells had a C-terminal fusion peptide containing an enterokinase cleavage site and a His-tag [9,10,18]. The new mutant, 1A9/Y483D, carried an identical C-terminal extension and, hence, the activities of the mutated enzyme could be directly compared to those of the His-tagged UGT1A9.

The relative amounts of UGT1A9 and 1A9/Y483D in the respective membrane fractions were estimated by immuno-labelling, in which the chemiluminescence was measured directly from the nitrocellulose membrane by a sensitive camera inside the detector/analyser (see Section 2), rather than by densitometry of a film that had been exposed to the membrane. The results showed that the Y483D mutation exerted no remarkable effect on the enzyme's expression. The concentration of 1A9/Y483D per milligram of membrane protein was lower than that of the control enzyme, UGT1A9, by about 15% (Fig. 1). It may be pointed out that we have used Dot blot analysis rather than Western blotting, mainly because, in this way, the possible problem of incomplete transfer of large membrane proteins from the acrylamide gel to the nitrocellulose membrane is overcome, and it also simplifies analyses of multiple samples. Dot blot analyses of the human UGTs are not, however, always feasible due to cross-reactivity of the antibodies with other proteins in the samples. The presence of six His residues at the C-terminal of these recombinant UGTs was valuable in this respect, since it allowed the use of monoclonal anti-His-tag antibodies. These antibodies were highly specific and did not cross-react significantly with other proteins in Western blot analyses of the membranes or membrane extracts [9].

The activities of 1A9/Y483D towards scopoletin (Fig. 2A) and entacapone (Fig. 2B) were analysed and compared to the corresponding activities of the UGT1A9. The kinetic constants that were derived from these experiments are summarised in Table 1. It also includes the corrected (normalized) V_{max} values for 1A9/Y483D that take into account the relative expression level of the mutant (Fig. 1). Tyr483 is located deep inside the C-terminal half of the UGT1A9, and this domain is largely assumed to harbour

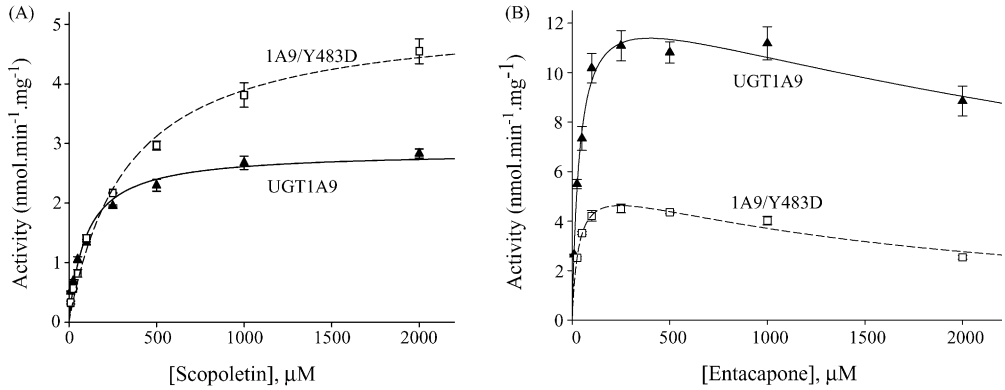

Fig. 2. Kinetic analyses of scopoletin (A) and entacapone (B) glucuronidation by UGT1A9 (black triangles, solid lines), and the mutant 1A9/Y483D (open squares, dashed lines). The curves show fitting of the scopoletin glucuronidation kinetics data to the Michaelis–Menten equation (Fig. 2A) whereas the entacapone data (Fig. 2B) were fitted to the substrate inhibition equation (see Section 2, $n = 3$).

the UDP-GA binding site. Due to this, we have also examined the kinetics of the mutant and the control enzymes with respect to UDP-GA, using scopoletin as the aglycone acceptor, and the derived K_m values are presented in Table 1.

The activity and kinetics results clearly show that in sharp contrast to the previous results with UGTs 1A1 and 1A6 [14], the Y483D mutation increased the activity of UGT1A9, at least as far as scopoletin glucuronidation is concerned (Fig. 2A, Table 1). It may be argued that different expression systems employed were the reason for the apparent difference between the current results with UGT1A9 and the previous results with UGTs 1A1 and 1A6. In order to exclude this possibility, we have prepared the corresponding mutant in UGT1A6, 1A6/Y485D that carries the same C-terminal fusion peptide as 1A9/Y483D, and expressed it in baculovirus-infected insect cells. In this case, after taking the expression level into account, the scopoletin glucuronidation rate of the 1A6/Y485D mutant was merely about 1% of the respective activity of UGT1A6 (data not shown). Hence, the difference in the effect of this Y to D mutation between UGT1A9 to UGT1A6 is remarkable also when both enzymes are expressed in the same system, and assayed for the same activity.

Table 1
Kinetic parameters for scopoletin and entacapone glucuronidation by UGT1A9 and the mutant 1A9/Y483D

	UGT1A9	1A9/Y483D
Scopoletin		
K_m (μM)	97 ± 10	328 ± 28
V_{max} (pmol min^{-1} mg^{-1})	2865 ± 75	5174 ± 146
Normalized V_{max}	2865	6087
Entacapone		
K_m (μM)	38 ± 6	34 ± 4
V_{max} (pmol min^{-1} mg^{-1})	13575 ± 714	5900 ± 245
Normalized V_{max}	13575	6940
UDP-GA (Scopoletin)		
K_m (μM)	423 ± 50	962 ± 88

The kinetic parameters for scopoletin and entacapone glucuronidation were derived from the data in Fig. 2A and B, respectively. The UDP-GA concentration in these assays was 5 mM. The K_m for UDP-GA was determined in a set of assays, in which the aglycone was 0.5 mM scopoletin. The kinetic parameters and their standard errors ($n = 3$) were calculated using the SigmaPlot package (enzyme kinetics module 1.1). The normalized V_{max} are corrected according to the relative expression level of the enzyme per mg membrane protein (Fig. 1).

In contrast to its effect on the activity of UGT1A9 towards scopoletin, however, the Y483D mutation lowered the V_{max} of entacapone glucuronidation (Fig. 2B, Table 1). This means that the mutation affected the scopoletin and entacapone glucuronidation activities of UGT1A9 in different and opposite ways, thereby decreasing the ratio of entacapone to scopoletin glucuronidation rates (V_{max}'s, Table 1) by about four-fold. Interestingly, the change in this ratio of activities, although not the extent, resembles the effect of UGT1A9 truncation six residues downstream the point of the Y483D mutation [10].

The differences in the effect of Tyr to Asp mutation between UGT1A9 and UGT1A6 may best be explained by differences in the interactions of the N-terminal half with the C-terminal half. However, since the UGTs are dimeric enzymes [5–9], one may ask whether the interaction between these two major domains of the UGTs is inside the same polypeptide (intra-monomeric) or between opposite monomers (inter-monomeric)? It may further be asked if the trans-membrane helix play a major role in these interactions? The truncation mutant 1A9Sol appears to be a useful tool for addressing this subject, e.g. by trying to prepare hetero-dimeric UGTs, in which one of the partners, 1A9Sol, lacks the trans-membrane helix and the cytoplasmic tail. In this respect, it should be noted that the ratio of entacapone to scopoletin glucuronidation rates in the 1A9Sol was below 0.1, whereas in full-length and membrane-bound UGT1A9 it was about 4 (Table 1, [10]). Therefore, a significant increase in this ratio of activities upon the generation of hetero-dimers would indicate functional inter-monomeric interactions between the participating UGTs, provided that both of the measured activities in the tested cells are exclusively catalysed by 1A9Sol. Accordingly, we have selected UGT1A4 to be the second partner in the hetero-dimerization experiments, since it

glucuronidates neither scopoletin nor entacapone at significant rates (see below).

The methodology we adopted was generating hetero-dimers by infecting insect cells with mixtures of recombinant baculoviruses that encode either 1A9Sol or UGT1A4. This implies that in addition to the desired hetero-dimers, the co-infected cells will also contain homo-dimers of each type. However, since UGT1A4 homo-dimers will be virtually silent in the activity assays, it was advantageous to try and increase the relative amount of hetero-dimers in comparison to 1A9Sol homo-dimers, even if this would increase the homo-dimerization of UGT1A4. It should also be considered that we could not (and cannot) assume that the tendency of a newly synthesised 1A9Sol to form a dimer with another 1A9Sol monomer is equal to its tendency to form a hetero-dimer with a newly synthesised UGT1A4. Nevertheless, it is reasonable to assume that lowering the number of newly synthesised 1A9Sol and concomitantly increasing the number of newly synthesised UGT1A4 would raise the probability of forming hetero-dimers and, subsequently, increase the ratio of entacapone to scopoletin glucuronidation rates. Accordingly, we have conducted a series of co-infections, using different proportions of the two recombinant baculoviruses in each case, as detailed in Fig. 3.

The scopoletin and entacapone activities in the co-infected cells were tested on suspensions of washed and frozen-thawed cells, and the results show that the activities, particularly entacapone glucuronidation, were strongly influenced by the composition of the infection mixture (Fig. 3). Since the cells that were infected only with UGT1A4 were virtually inactive in the glucuronidation of both, scopoletin and entacapone (Fig. 3), the increase in

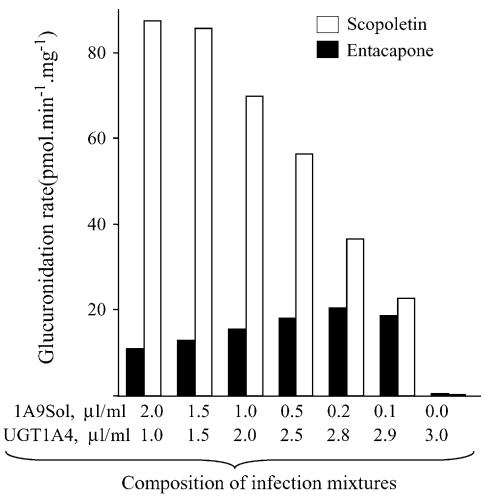

Fig. 3. Co-infection with UGT1A4 increases the entacapone glucuronidation activity of 1A9Sol. Insect cells were infected by a fixed volume (3 μl per 1 ml cell suspension) of different proportions of recombinant baculoviruses encoding either 1A9Sol [10], or UGT1A4 (1A4XHC, [9]). The fraction of each UGT in the infection mixture is shown below the abscissa. Entacapone glucuronidation rates are denoted by black bars, and scopoletin glucuronidation rates by open bars.

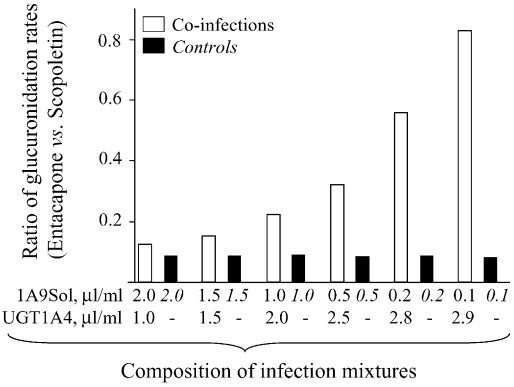

Fig. 4. The dependence of the ratio of entacapone to scopoletin glucuronidation rates on the composition of the co-infection mixture. The ratio of these activities in co-infected and control cells (open and black bars, respectively) is shown on the ordinate, and the baculovirus mixtures that were used to infect the cells are indicated below the abscissa.

entacapone glucuronidation rates upon raising the proportion of UGT1A4 in the infection mixture was, almost certainly, due to the formation of 1A9Sol-UGT1A4 hetero-dimers.

The ratio of entacapone to scopoletin glucuronidation rates was convincingly dependent on the proportion of 1A9Sol and UGT1A4 in the infection mixtures (Fig. 4). The controls for the co-infected samples were infections with the corresponding amount of 1A9Sol-encoding baculovirus, but without the UGT1A4. The results reveal that in the co-infected cells, there was a very clear correlation between increasing the probability of forming 1A9Sol-UGT1A4 hetero-dimers, and the rise in the ratio of entacapone to scopoletin glucuronidation rates (Fig. 4, open bars). In the control samples, on the other hand, that ratio of activities was independent of the infection size (Fig. 4, black bars).

The effect of hetero-dimerization on the catalytic properties of 1A9Sol was also examined at the level of enzyme kinetics. Since the entacapone glucuronidation rate of 1A9Sol homo-dimers is low [10], it could be safely assumed that in the cells that were infected with the lowest relative proportion of 1A9Sol and exhibited the highest ratio of activities (Fig. 4), nearly the entire entacapone glucuronidation was catalysed by 1A9Sol that was present in hetero-dimers with UGT1A4. Hence, the cells that had been infected with the virus mixture of 0.1:2.9 (1A9Sol:UGT1A4), were subjected to kinetic analysis of entacapone glucuronidation, and the results indicated that the co-infection reduced the apparent K_m of 1A9Sol to entacapone by about nine times to 52 μM (Fig. 5). Notably, the latter value is very similar to the apparent K_m for entacapone in the full-length and membrane-bound UGT1A9 (Fig. 2B, Table 1, and [10]). It thus appears that the truncated enzyme 1A9Sol functionally interacted with the full-length UGT1A4, an interaction that significantly affected its kinetic properties.

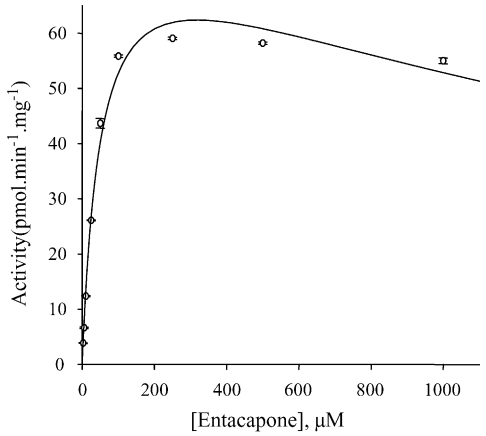

Fig. 5. Glucuronidation kinetics of entacapone in insect cells that were co-infected with a mixture containing 0.1 μl 1A9Sol and 2.9 μl UGT1A4 per 1 ml of cell suspension (the lowest proportion of 1A9Sol in comparison to UGT1A4 among the co-infected samples in Fig. 3. The experimental data were fitted to the substrate inhibition equation (see Section 2), and the derived K_m was 52 ± 13 μM (the value of V_{max} in this sample was 83 ± 11 pmol min^{-1} mg^{-1}).

It would have been interesting to examine if the co-infection with UGT1A4 also changes the kinetics of 1A9Sol in scopoletin glucuronidation, or the ratio of scopoletin to entacapone glucuronidation rates of the 1A9/Y483D. Unfortunately, at present, we have neither a way to prevent the homo-dimerization nor a reliable and accurate method to determine the relative amounts of homo- and hetero-dimers in the co-infected cells. Hence, co-infection is a useful method when the partners have very low activity towards a given substrate, entacapone in the cases of 1A9Sol and UGT1A4. On the other hand, when scopoletin glucuronidation kinetics of the same sample is analysed there is a significant, and perhaps even a dominant, contribution from 1A9Sol dimers that readily glucuronidate scopoletin, thereby rendering such an analysis meaningless.

4. Discussion

Each of the UGTs can be divided into two large and almost equal size sections, namely the N-terminal half that is likely to play a major role in the aglycone binding, and the highly conserved C-terminal half that probably harbours the UDP-GA binding site. Interactions between these domains may be necessary for the structure and the function of these enzymes. For example, they might bring the glucuronic acid moiety of the bound UDP-GA into the vicinity of the sugar-accepting group on the aglycone. In this respect, it may be noted that previous affinity labelling experiments suggested that the sugar part of the UDP-GA may be bound by the N-terminal half of the UGT, whereas the nucleotide was bound within the C-terminal half [19]. In the current study, we have first tried to examine whether or not such interactions are isoform-specific, since this may be among the factors that determine substrate specificity and kinetic variations among the UGTs. The alternative and perhaps more expected assumption at the outset of this study was that due to the primary structure identity of the C-terminal domain among all the UGT1As, and the considerable degree of similarity in their N-terminal region, the domains' interaction is nearly identical in all the isoforms.

The 1A1/Y486D mutation was previously reported to inhibit UGT1A6 even more than 1A1 [14], and could therefore point towards isoform-specific differences in domains' interactions among the UGTs of the 1A subfamily. We have thus generated the 1A9/Y483D mutant and studied its glucuronidation activity towards scopoletin and entacapone (Fig. 2, Table 1). The results demonstrated that in sharp contrast to the effect of this mutation on either UGT1A1 or UGT1A6, the corresponding mutation in UGT1A9 increased rather than inhibited the rate of activity, at least as far as scopoletin glucuronidation was concerned (Fig. 2A). We have carefully examined the effect of the mutation on protein expression (Fig. 1), and verified that the difference between UGT1A9 and UGT1A6 is neither due to the expression system, nor due to the use of scopoletin as the aglycone substrate in the present studies (see above). Hence, the difference in the effect of the Y483D mutation (Y485D in UGT1A6) between the human UGTs 1A9 and 1A6, the C-terminal half of both is identical at the level of amino acid sequence, must have emerged from differences within the N-terminal half. Therefore, since the mutation is located deep inside the C-terminal half, the results reveal that there are important protein–protein interactions between the region that is located immediately upstream the beginning of the trans-membrane helix and the N-terminal half.

Considering interactions between the N-terminal half and the C-terminal half of the UGTs, one may ask whether the interacting domains are located on the same monomer, or are they segments of opposite monomers within the dimeric UGT? The latter possibility implies that there are functional monomer–monomer interactions and in order to test this hypothesis, we have prepared hetero-dimers containing 1A9Sol and UGT1A4. The working hypothesis was that the intact C-terminal half of UGT1A4 could interact with the N-terminal half of 1A9Sol, thereby modifying its catalytic properties, and at least partly restoring the activity characteristics of full-length UGT1A9. Hetero-dimerization was induced by co-infection, and the activities and kinetic results were in agreement with the expectations, and even surpassed them. Hence, in comparison to cells infected with 1A9Sol alone, there was a significant increase in the ratio of entacapone versus scopoletin glucuronidation rates (Fig. 4), and the direction of the change was towards the corresponding value in the full-length and membrane-bound UGT1A9 (Fig. 2, Table 1, and [10]). Significantly, the dependence of the entacapone glucuronidation rate on the probability of generating het-

ero-dimers, was a strong evidence that it has originated from the 1A9Sol that is functionally interacting with the UGT1A4 (Fig. 3).

The ratio of entacapone to scopoletin glucuronidation rate was not, however, the only way in which monomer–monomer interactions were examined. The second parameter was the kinetics of entacapone glucuronidation, mainly its apparent K_m, since this value in 1A9Sol was about 10 times higher than in UGT1A9 [10]. The results of this analysis (Fig. 5), when compared to 1A9Sol alone [10], clearly showed that the hetero-dimerization with UGT1A4 affected to the kinetics of entacapone glucuronidation. Moreover, the apparent K_m for entacapone in the hetero-dimers (Fig. 5) is very close to that in full-length and membrane-bound UGT1A9 (Fig. 2B, Table 1, [10]). These results provide an additional support for the formation of functional hetero-dimers containing UGT1A4 and 1A9Sol, and since the latter lacks the trans-membrane helix and the cytoplasmic tail, it may be concluded that they are not essential for these protein–protein interactions.

It was previously shown that UGT1A9 is much more resistant to Triton X-100 solubilization than most other human UGTs [9], and in sharp contrast to UGT1A6, truncation of UGT1A9 immediately above the start of the trans-membrane helix generates a water-soluble and at least partly active enzyme [10]. The site of the Y483 mutation is very close to the point of truncation in 1A9Sol and, thus, the results of the current study about the differences in the consequences of this Y to D mutation between UGT1A9 and UGT1A6 might be reminiscent of the previous results. Nevertheless, UGTs 1A9 and 1A6 are homologous to each other, and it might be a mistake to presume that these enzymes are entirely different in their structure–function relationships. In this respect, it is worth pointing out that the resistance of UGT1A9 to detergent inhibition was only partial, limited to merely few aglycones, and even in these cases, it affected the enzyme kinetics [9]. It is likely that due to one or few amino acid substitutions in the N-terminal half of the enzyme, UGT1A9 is more stable than UGT1A6 in the absence of the trans-membrane helix, or when it is affected by bound detergent. This additional stability, that could arise from small differences in protein–protein interactions, made UGT1A9 instrumental in studying the features that are not easily explored with other UGTs. Nevertheless, the results may be generally applicable to most other UGTs.

The current results do not prove that the N-terminal half of the truncated 1A9Sol is interacting directly with the C-terminal half of the intact UGT1A4. However, taking the results of the current study into account, it is tempting to suggest that this is indeed the situation within the hetero-dimers. This suggestion is compatible with previous studies about dimeric UGTs, including the involvement of the very N-terminus of the mature protein in dimerization [5], and the dominant-negative effect of some UGT1A1 mutants on the activity [7].

In conclusion, this study has revealed extended and isoform-specific protein–protein interactions within the dimeric UGTs. Further work is clearly needed for better characterization and mapping of these interactions, and exploring their possible contribution to the complex substrate-specificity of the UGTs.

Acknowledgements

We thank Johanna Mosorin, Saila Mörsky and Sanna Sistonen for skilful technical assistance. This research was supported by the Academy of Finland (Project No. 207535) and the National Technology Agency, Finland.

References

[1] Meech R, Mackenzie PI. Structure and function of uridine diphosphate glucuronosyltransferases. Clin Exp Pharmacol Physiol 1997;24:907–91.
[2] Radominska-Pandya A, Czernik PJ, Little JM, Battaglia E, Mackenzie PI. Structural and functional studies of UDP-glucuronosyltransferases. Drug Metab Rev 1999;31:817–99.
[3] Tukey RH, Strassburg CP. Human UDP-glucuronosyltransferases: metabolism, expression and disease. Annu Rev Pharmacol Toxicol 2000;40:581–616.
[4] Ouzzine M, Barre' L, Netter P, Magdalou J, Fournel-Gigleux S. The human UDP-glucuronosyltransferases: structural aspects and drug glucuronidation. Drug Metab Rev 2003;35:287–303.
[5] Meech R, Mackenzie PI. UDP-glucuronosyltransferase, the role of the amino terminus in dimerization. J Biol Chem 1997;272:26913–7.
[6] Ikushiro S, Emi Y, Iyanagi T. Protein–protein interactions between UDP-glucuronosyltransferase isozymes in rat hepatic microsomes. Biochemistry 1997;36:7154–61.
[7] Ghosh SS, Sappal BS, Kalpana GV, Lee SW, Chowdhury JR, Chowdhury NR. Homodimerization of human bilirubin-uridine-diphosphoglucuronate glucuronosyltransferase 1 (UGT1A1) and its functional implications. J Biol Chem 2001;276:42108–15.
[8] Ishii Y, Miyoshi A, Watanabe R, Tsuruda K, Tsuda M, Yamaguchi-Nagamatsu Y, et al. Simultaneous expression of guinea pig UDP-glucuronosyltransferase 2B21 and 2B22 in COS-7 cells enhances UDP-glucuronosyltransferase 2B21-catalyzed morphine-6-glucuronide formation. Mol Pharmacol 2001;60:1040–8.
[9] Kurkela M, Garcia-Horsman JA, Luukkanen L, Mörsky S, Taskinen J, Baumann M, et al. Expression and characterization of recombinant human UDP-glucuronosyltransferases (UGTs). UGT1A9 is more resistant to detergent inhibition than other UGTs and was purified as an active dimeric enzyme. J Biol Chem 2003;278:3536–44.
[10] Kurkela M, Mörsky S, Hirvonen J, Kostiainen R, Finel M. An active and water-soluble truncation mutant of the human UDP-glucuronosyltransferase 1A9. Mol Pharmacol 2004;65:826–31.
[11] Aono S, Yamada Y, Keino H, Hanada N, Nakagawa T, Sasaoka Y, et al. Identification of defect in the genes for bilirubin UDP-glucuronosyltransferase in a patient with Crigler–Najjar syndrome type II. Biochem Biophys Res Commun 1993;197:1239–44.
[12] Kraemer D, Klinker H. Crigler–Najjar syndrome type II in a caucasian patient resulting from two mutations in the bilirubin uridine 5′-diphosphate-glucuronosyltransferase (UGT1A1) gene. J Hepatol 2002;36:706–7.
[13] Yamamoto K, Sato H, Fujiyama Y, Doida Y, Bamba T. Contribution of two missense mutations (G71R and Y486D) of the bilirubin UDP glycosyltransferase (UGT1A1) gene to phenotypes of Gilbert's syn-

drome and Crigler–Najjar syndrome type II. Biochim Biophys Acta 1998;1406:267–73.

[14] Ito M, Yamamoto K, Maruo Y, Sato H, Fujiyama Y, Bamba T. Effect of a conserved mutation in uridine diphosphate glucuronosyltransferase 1A1 and 1A6 on glucuronidation of a metabolite of flutamide. Eur J Clin Pharmacol 2002;58:11–4.

[15] Ouzzine M, Magdalou J, Burchell B, Fournel-Gigleux S. An internal signal sequence mediates the targeting and retention of the human UDP-glucuronosyltransferase 1A6 to the endoplasmic reticulum. J Biol Chem 1999;274:31401–9.

[16] Meech R, Yogalingam G, Mackenzie PI. Mutational analysis of the carboxy-terminal region of UDP-glucuronosyltransferase 2B1. DNA Cell Biol 1996;15:489–94.

[17] Luukkanen L, Kilpelainen I, Kangas H, Ottoila P, Elovaara E, Taskinen J. Enzyme-assisted synthesis and structural characterization of nitrocatechol glucuronides. Bioconjug Chem 1999;10: 150–4.

[18] Kuuranne T, Kurkela M, Thevis M, Schänzer W, Finel M, Kostiainen R. Glucuronidation of anabolic androgenic steroids by recombinant human UDP-glucuronosyltransferases. Drug Metab Dispos 2003;31: 1117–24.

[19] Pillot T, Ouzzine M, Fournel-Gigleux S, Lafaurie C, Tebbi D, Treat S, et al. Determination of the human liver UDP-glucuronosyltransferase 2B4 domains involved in the binding of UDP-glucuronic acid using photoaffinity labeling of fusion proteins. Biochem Biophys Res Commun 1993;197:785–91.